Blocked Enzymatic Etching of Gold Nanorods: Application to Colorimetric Detection of Acetylcholinesterase Activity and its Inhibitors

*Laura Saa[a], Ruta Grinyte[a], Ana Sánchez-Iglesias[a], Luis M. Liz-Marzán[a,b,c *], Valeri Pavlov[a*]*

[a] *CIC biomaGUNE, Paseo de Miramón 182, 20009 Donostia - San Sebastián, Spain*

[b] *Ikerbasque, Basque Foundation for Science, 48011 Bilbao, Spain*

[c] *Biomedical Research Networking Center in Bioengineering Biomaterials and Nanomedicine, Ciber-BBN, Spain*

KEYWORDS

Gold nanorods; Enzymatic biosensing; Nerve gases; etching; acetylcholinesterase.

ABSTRACT

The anisotropic morphology of gold nanorods (AuNRs) has been shown to lead to non-uniform ligand distribution and preferential etching through their tips. We have recently demonstrated that this effect can be achieved by biocatalytic oxidation with hydrogen peroxide, catalyzed by the enzyme horseradish peroxidase (HRP). We report here that modification of AuNRs with thiol-containing organic molecules such as glutathione and thiocholine hinders enzymatic AuNR etching. Higher concentrations of thiol-containing molecules in the reaction mixture gradually decrease the rate of enzymatic etching, which can be monitored by UV-Vis spectroscopy, through changes in the AuNR longitudinal plasmon band. This effect can be applied to develop novel optical assays for acetylcholinesterase (AChE) activity. The biocatalytic hydrolysis of acetylthiocholine by AChE yields thiocholine, which prevents enzymatic AuNR etching in the presence of HRP. Additionally, the same bioassay can be used for the detection of nanomolar concentrations of AChE inhibitors such as paraoxon and galanthamine.

Introduction

The physical properties of inorganic nanoparticles (NPs) depend on their shape, size and composition.[1] Noble metal NPs exhibit strong localized surface plasmon resonances (LSPR) in the visible or near-IR wavelength range. Hence, metal NPs of different nature have found broad application in imaging and colorimetric bioanalytical assays.[2-4] Metal NPs of different shapes have been reported[5] and gold nanorods (AuNRs) in particular have recently found wide application in bioanalysis.[6-8] AuNRs can be employed as a highly sensitive platform to probe environmental changes through variations in their length because the longitudinal LSPR frequency is highly sensitive to minute changes in the AuNR aspect ratio.[8-10] Post-synthetic morphological modifications of AuNRs leading to detectable LSPR changes have been reported, including shortening,[11] lateral etching,[12] and transverse overgrowth.[13] Shortening of AuNRs can be achieved by oxidation of Au^0 atoms in aqueous solutions containing high concentrations of hydrogen peroxide.[14] Such an oxidation process occurs in acidic solutions at high temperature. Such harsh experimental conditions are however incompatible with most bio-analytical applications. In an attempt to mitigate this issue, metal ions (Cu^{2+}, Pb^{2+}, Fe^{3+}, Cr(VI)) were employed as catalysts for the oxidation of gold NPs.[7, 15-18] Another approach to etching of AuNRs under physiological conditions relies on enzymatic Au^0 oxidation catalyzed by the redox enzyme horseradish peroxidase (HRP).[8] The use of HRP instead of metal cations (which in some cases denature proteins and inhibit enzymes) enables extending the set of biorecognition elements used in bioanalysis in conjugation with AuNRs.

AuNRs are usually synthesized by seed-mediated growth in water, in the presence of a shape-directing surfactant, cetyltrimethylammonium bromide (CTAB).[19] It has been postulated that the packing density of CTAB is higher along the side facets of AuNRs, leaving more exposed the

facets at the tips.[20] Numerous reports thus demonstrate that thiol-containing organic molecules preferentially bind to AuNR tips.[20-23] Accordingly, the oxidative shape transformation of CTAB-stabilized AnNRs results in shortening that starts at the tips.[8, 11, 23] In this context, organic thiols such as glutathione and thiocholine are expected to prevent enzymatic etching of CTAB-stabilized AuNRs catalyzed by HRP, in a concentration dependent manner, which can be exploited as a novel biodetection assay.

Thiocholine is the product of the enzymatic hydrolysis of the artificial enzymatic substrate acetylthiocholine, catalyzed by acetylcholine esterase (AChE). In Nature this enzyme breaks down acetylcholine at cholinergic synapses, gaps where a neuron that produces acetylcholine sends messages to other neurons, or to skeletal muscle cells. The recipient cells adsorb acetylcholine from cholinergic synapses. Neurons continually produce acetylcholine during communication; therefore this compound should be enzymatically decomposed in the synapse after use to prevent the continuous activation of cells. In the presence of inhibitors, AChE is not able to clear acetylcholine from the synapse and thereupon the accumulation of this neurotransmitter throughout the body affects the physiology of the nervous system with serious or fatal consequences.[24] Some AChE inhibitors are employed as chemical warfare agents (nerve gases) or pesticides, which prevent muscle contractions assisting in breathing of living beings. Lethal nerve agents are hazardous to humans and livestock hence in the past decade many efforts have been made to develop sensitive and efficient methods to detect AChE inhibitors in air, water and food. In this manuscript we report the protective effect of thiol-containing compounds against enzymatic etching of AuNRs and application of this phenomenon to the development of a simple optical bioassay for the enzymatic activity of AChE and sensitive detection of AChE inhibitors.

Experimental Section

Materials. Tetrachloroauric acid ($HAuCl_4$), sodium borohydride ($NaBH_4$), silver nitrate ($AgNO_3$), hexadecyltrimethylammonium bromide (CTAB), hydrochloric acid (HCl) and L-ascorbic acid (AA), acetylthiocholine chloride (ATCh), acetylcholinesterase from electric eel, horseradish peroxidase type VI, diethyl p-nitrophenyl phosphate (Paraoxon), galanthamine hydrobromide (from Lycoris Sp.) and other chemicals were purchased from Sigma-Aldrich. All reactants were used without further purification. Milli-Q water was used in all experiments. Absorbance measurements were performed in a Varioskan Flash microplate reader (Thermo Scientific) using 96-microwell plates. The UV-Vis absorbance spectra were scanned from 400 to 900 nm at RT.

Synthesis of gold nanorods. Gold nanorods were prepared using Ag-assisted seeded growth.[25, 26] Seeds were prepared by reduction of $HAuCl_4$ (0.25 mM, 5 mL) with freshly prepared $NaBH_4$ (10 mM, 0.3 mL) in aqueous CTAB solution (100 mM). After 30 minutes, an aliquot of seed solution (0.55 mL) was added to a growth solution (250 mL) containing CTAB (100 mM), $HAuCl_4$ (0.5 mM), ascorbic acid (0.8 mM), $AgNO_3$ (0.12 mM), and HCl (19 mM). The mixture was left undisturbed at 30 °C for 2h. The solution was centrifuged twice (8000 rpm, 30 min) to remove excess silver salt, ascorbic acid, CTAB and HCl, and redispersed in CTAB (100 mM).

Characterization. TEM images were obtained with a JEOL JEM-1400PLUS transmission electron microscope operating at an acceleration of 120kV. UV-Vis spectra were measured with an Agilent 8453 UV-Vis spectrophotometer.

Effect of thiols on the rate of enzymatic AuNR etching. The etching assay was performed by adding 3.5 μL of AuNRs ([Au^0]=2.97 mM in 0.1 M CTAB), 1 μL of HRP (120 μM in citrate buffer 0.2 M pH 4.0), 1 μL of HCl (0.5 M) and 2.8 μL of H_2O_2 (1.76 mM) to solutions (90 μL) containing different concentrations of reduced glutathione or enzymatically produced thiocholine. Absorbance spectra of the resulting mixtures were recorded after 15 min.

Detection of acetylcholinesterase. Acetylthiocholine chloride (0.02 mM) was incubated with different amounts of AChE in 10 mM Tris-HCl buffer (pH 7.4) in a final volume of 90 μL, at RT for 25 min. The etching assay was then performed as described above and absorbance spectra of the resulting mixtures were recorded after 15 min.

Inhibition of AChE by Paraoxon and Galanthamine. Different concentrations of inhibitor were incubated with 1.4 mU mL^{-1} AChE in 10 mM Tris-HCl buffer (pH 7.4), in a final volume of 85 μL, at RT for 1 h. Next, 5 μL of 0.4 mM acetylthiocholine chloride in 10 mM Tris-HCl buffer (pH 7.4) was added, and the resulting mixture was incubated at RT for 25 min. Thereafter, the etching assay was performed as described above and absorbance spectra of the resulting mixtures were recorded after 15 min.

Quantification of acetylcholinesterase in human serum. Commercial human serum was spiked with different concentrations of acetylcholinesterase and the concentration of the mixtures was determined as described above. The dilution factor of serum in the assay was 1:20000.

Results and Discussion

Effect of thiols on the rate of biocatalytic etching of gold nanorods

We have recently demonstrated that the enzyme horseradish peroxidase catalyzes oxidative anisotropic etching of CTAB capped AuNRs in the presence of hydrogen peroxide acting as an oxidizer and bromide acting as a gold complexing agent. [8] The surface of Au NRs stabilized with CTAB is different from that of spherical Au NPs. Micelles composed of CTAB complexed with AgBr (CTAB-AgBr) confine the geometry of Au growth and stabilize the lateral facets on the nanorod surface. It has been reported[27] that the axis of AuNRs is orientated along the [001] direction and the side faces consist of eight equal high-index {520} facets. A complex between CTAB and AgBr selectively stabilizes {520} side facets during the synthesis of AuNRs while the tips consist of a combination of {110}, {100}, and {111} facets. Because of differences in surface energy,[28] the lateral faces are more likely to accommodate the heads and tails of the CTAB-AgBr complex, whereas the interaction of CTAB-AgBr with {110}, {100} and {111} surfaces is less effective. Gold atoms on tip facets {110}, {100}, {111} thus form weaker bonds with the surfactant and the surface coverage of CTAB-AgBr is lower as compared to that on the side faces. This explains why the enzymatic oxidation of AuNRs starts at the more exposed tips, resulting in shortening of the rods and leading to detectable changes in their longitudinal LSPR

band. Interestingly, we found that the rate of biocatalytic etching of AuNRs can be modulated by the presence of thiols in the reaction mixture.

Figure 1A displays longitudinal LSPR bands recorded after HRP-catalyzed oxidative etching of AuNRs for 15 min, in the presence of varying concentrations of glutathione (GSH) and the fixed concentration of 50 μM of H_2O_2 which is optimum for reproducible monitoring of LSPR shift. According to Figure 1B, where the LSPR position is plotted vs. GSH concentration, increasing amounts of thiol in the reaction mixture lead to a smaller effect of enzymatic etching on the length of the AuNRs. The corresponding calibration curve exhibits linearity from 0 to 1 μM, as well as a saturation segment starting from a GSH concentration of 7 μM. The shape of the curve indicates that the kinetics of GSH binding to AuNRs obeys the Langmuir adsorption isotherm model:

$$[GSH]/\Delta\lambda = K_d/\Delta\lambda_{max} + [GSH]/\Delta\lambda_{max} \qquad (1)$$

where [GSH] is GSH concentration, $\Delta\lambda$ is the difference LSPR-$LSPR_{[GSH]=0.0}$, and $\Delta\lambda_{max}$ is $LSPR_{max}$-$LSPR_{[GSH]=0.0}$. Using this equation and nonlinear regression fitting, the apparent dissociation constant, K_d, between GSH and AuNRs was found to be 2.6 ± 0.3 μM.

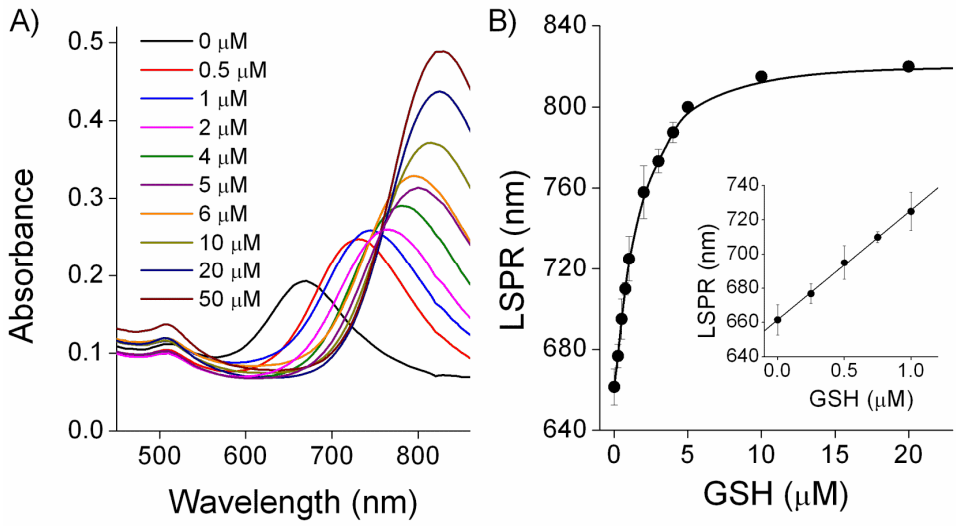

Figure 1. Influence of GSH on the enzymatic etching of AuNRs. (A) Absorbance spectra recorded after the enzymatic etching of AuNRs preincubated with different concentrations of GSH. (B) LSPR shift as a function of GSH concentration. The solid line is a fit of a Langmuir isotherm model to the data. Inset: linear part of the calibration plot.

We also studied the impact of a second thiol of interest – thiocholine – on the rate of HRP-catalyzed AuNR etching. Longitudinal LSPR bands recorded after HRP-catalyzed etching of AuNRs in the presence of varying concentrations of thiocholine are presented in **Figure 2**. The plot of LSPR position *vs.* thiocholine concentration shows a linear segment up to 15 μM and saturation starting from 30 μM thiocholine (**Figure 1S** in Supporting Information). The shape of the plot indicates that the interaction of thiocholine with AuNRs also complies with the Langmuir adsorption isotherm model. The apparent dissociation constant, K_d, between thiocholine and AuNRs, equal to 12.0 ± 1.5 μM.

Control experiments in which the enzymatic activity of HRP was measured employing the standard chromogenic substrate 3,3',5,5'-tetramethylbenzidine (TMB), in the presence of thiocholine concentrations up to 60 μM (A) and in the range of GSH concentrations from 0 to 20 μM, (B) did not demonstrate any inhibiting effect of the thiol. under our experimental conditions (Figure 2S in Supporting information).

The protective effect of GSH and thiocholine against the biocatalytic oxidative etching of AuNRs is in agreement with the previous discussion in terms of thiol binding to the ends of nanorods, as shown in **Scheme 1**. Thiol molecules (R-SH) bind preferentially to {110}, {100}, {111} facets located at the tips of AuNRs where CTAB surface coverage is lower. Thiols compete with hydroxyl radicals for the exposed gold surface hence a higher surface concentration of protective thiol molecules at the AuNR tips will decrease the rate of enzymatic anisotropic oxidation of gold by hydroxyl radicals.

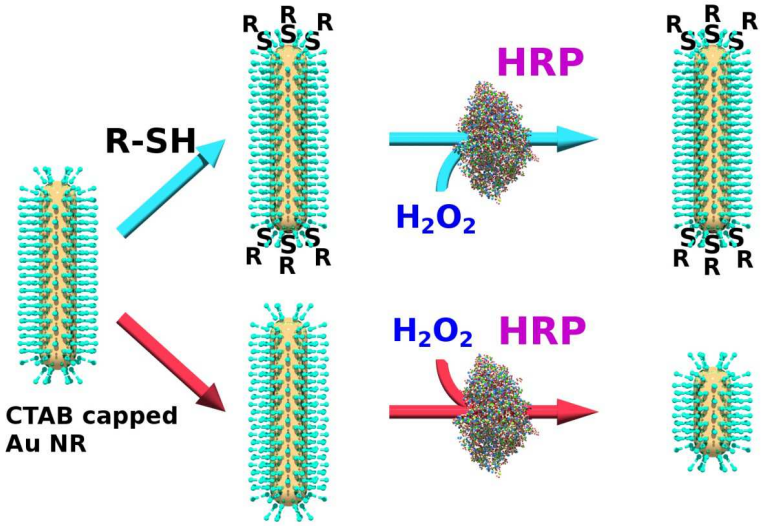

Scheme 1. Schematic illustration of the protective effect of thiol molecules (R-SH) against biocatalytic oxidative etching of AuNRs.

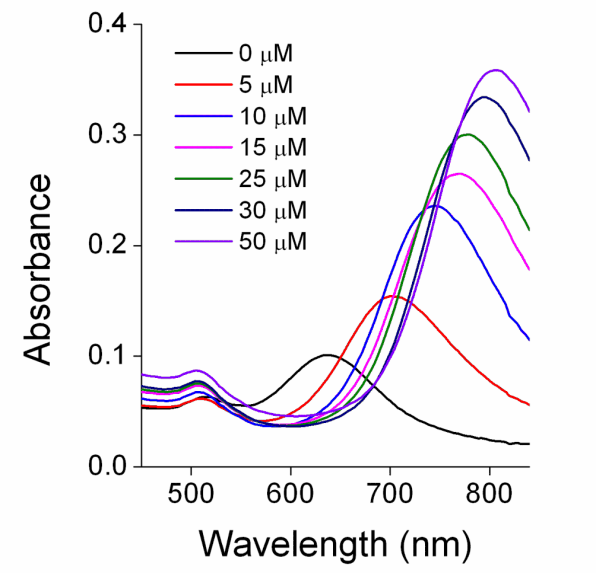

Figure 2. Influence of thiocholine on the enzymatic etching of AuNRs. Absorbance spectra recorded after the enzymatic etching of AuNRs for 15 min, preincubated with different concentrations of thiocholine.

Detection of acetylcholinesterase activity based on AuNR etching

We studied the dependence of the absorbance spectra (**Figure 3A**) and of LSPR position (**Figure 3B**) on increasing AChE concentrations using the ATCh fixed concentration (20 μM). According to the calibration plot in **Figure 3B**, curve **a**, the increase in AChE concentration leads to a red shift of the final LSPR position which is related to longer AuNRs remaining in the reaction mixture after oxidative etching catalyzed by HRP. According to the calibration curve, de detection limit was 0.04 mU/mL, which is lower than this obtained by the most relevant

previously published colorimetric methods employing growth of gold (26 mU/mL[29], 0.6 mU/mL[30]), silver NPs (0.1 mU/mL).[3] ,amine-terminated polydiacetylene vesicles[31](10 mU/mL) and the water-soluble polythiophene derivative (200 mU/mL)[32]

A control experiment was carried out to examine the effect of increasing AChE concentrations on the length of HRP-etched AuNRs in the absence of the enzymatic substrate ATCh (**Figure 3B**, curve **b**). The result confirms that AChE without ATCh can not protect AuNRs from enzymatic etching.

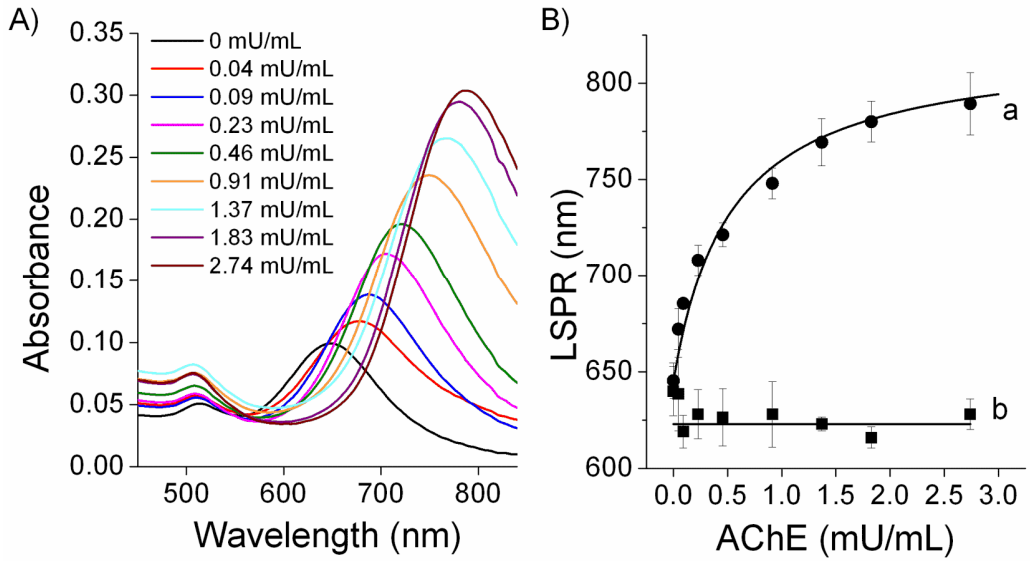

Figure 3. Influence of AChE on enzymatic etching of AuNRs. (A) Absorbance spectra recorded after enzymatic etching of AuNRs for 15 min, preincubated with ATCh (0.02 mM) and different concentrations of AChE. (B) LSPR shift as a function of AChE concentration, preincubated with (curve **a**) or without ATCh (curve **b**). The solid lines are guides to the eye.

As described in the previous section, low concentrations of thiocholine (below 5 μM) are able to impair the rate of AuNR etching catalyzed by HRP. Thiocholine can be enzymatically produced *in situ* by the enzyme AChE from the artificial substrate acetylthiocholine (ATCh). Therefore, the rate of enzymatic hydrolysis of ATCh by AChE will influence the rate of thiocholine formation and consequently the rate of biocatalytic etching of AuNRs catalyzed by HRP (**Scheme 2**). This system was thus applied to develop a colorimetric assay for the detection of AChE activity. The influence of varying concentrations of the enzymatic substrate ATCh on the registered absorbance spectra in the presence of a fixed concentration of AChE (1 mU mL^{-1}) is shown in **Figure 4A**.

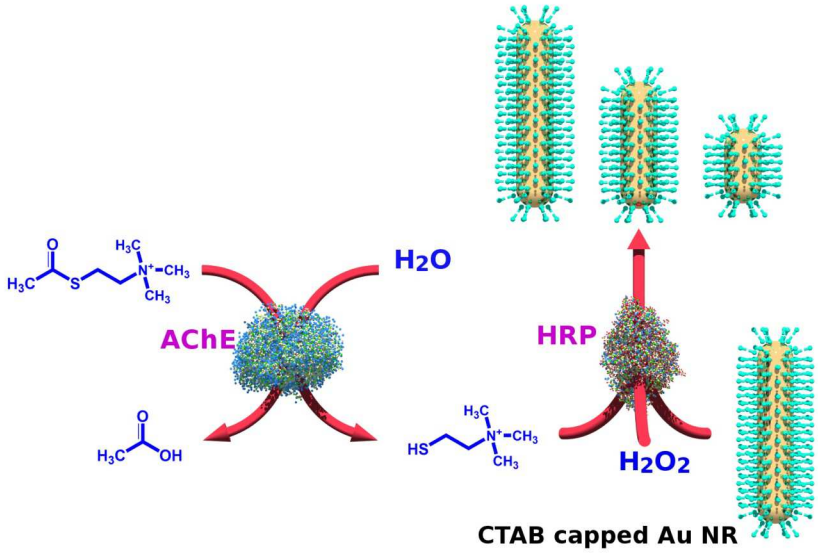

Scheme 2. System for detection of AChE activity based on enzymatically generated thiocholine modulating the rate of biocatalytic etching of AuNRs.

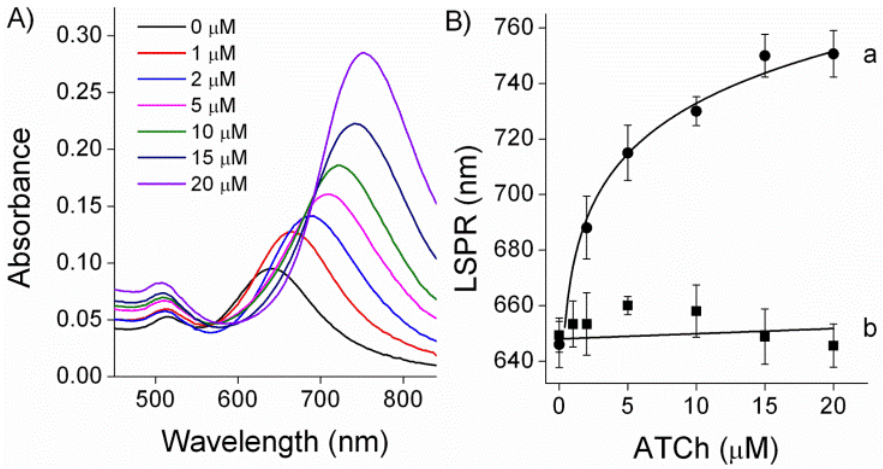

Figure 4. Influence of ATCh on AuNR enzymatic etching. (A) Absorbance spectra recorded after the enzymatic etching of AuNRs for 15 min, preincubated with AChE (1 mU/mL) and varying concentrations of thiocholine. (B) LSPR shift as a function of ATCh concentration preincubated with (curve **a**) or without AChE (curve **b**). The solid line in **a** is a fit of Michaelis-Menten equation to the data using the K_M equal to 0.1 mM and Figure 3 in order to relate LSPR shift with the enzymatic activity; the line in **b** is a guide to the eye.

The variation of LSPR position *vs*. ATCh concentration is presented in Figure 4B (curve **a**). In order to calculate the apparent Michaelis-Menten constant the equation (2) was employed

$$v = Vmax\,[S]/(K_M + [S]) \qquad (2)$$

where [S] is the concentration of ATCh, K_M is the apparent Michaelis-Menten constant, *Vmax* is the maximum rate of the enzymatic reaction and *v* is the reaction rate. The values of *v* corresponding to each concentration of substrate were calculated from the plot of LSPR vs. AChE concentration (Figure 3).

Non linear regression fitting to equation (2) of the obtained experimental data gave the value of K_M equal to 0.1 mM. This value is in good agreement with the value of Michaelis-Menten constant calculated under similar experimental conditions.[29]

Thus, the hydrolysis of ATCh catalyzed by AChE follows the classical Michaelis-Menten kinetic model with an initial bimolecular reaction between the enzyme and the substrate, interaction with water, and with the last irreversible step up to the total exhaustion of the substrate. Control experiments carried out with increasing concentrations of ATCh in the absence of AChE (**Figure 4A**, curve **b**) demonstrated no significant effect of the enzymatic substrate on the aspect ratio of AuNRs remaining in the reaction mixture after HRP-catalyzed etching.

The morphological changes of AuNRs upon HRP etching modulated by the AChE catalyzed generation of thiocholine were analyzed by TEM. The results show that the initial AuNRs were 50.5±1.8 nm long and 10.2±0.7 nm wide (**Figure 3S** in Supporting Information). AChE and the products of enzymatic hydrolysis of ATCh do not affect the shape and size of AuNRs (**Figure 4S** in Supporting Information). Only after the addition of HRP and hydrogen peroxide the decrease in the length of AuNRs was observed. TEM imaging of AuNRs obtained after oxidative etching in the presence of varying concentrations of AChE (**Figure 5**) revealed that the length of the resulting AuNRs is directly related to the amount of AChE in the system. The changes in AuNR length are reflected in visible changes in the color of the reaction mixtures from blue to brown. The plot of AuNRs length vs. AChE concentration (**Figure 5F**, curve **a**) reveals that, in the absence of AChE AuNRs become shorter by ca. 32 nm. In other words, AuNRs retain 38% of their initial length after HRP etching, in the absence of AChE. At AChE concentrations above 2.7 mU mL^{-1} AuNRs retain more than 90% of their initial length after biocatalytic etching. A

plot of AuNRs width vs. AChE concentration (**Figure 5F**, curve **b**) demonstrates that AChE activity, and consequently the amount of generated thiol, does not affect the diameter of etched AuNRs. This observation confirms our initial hypothesis that thiols preferentially bind to the tips of AuNRs, thereby protecting them against enzymatic shortening.

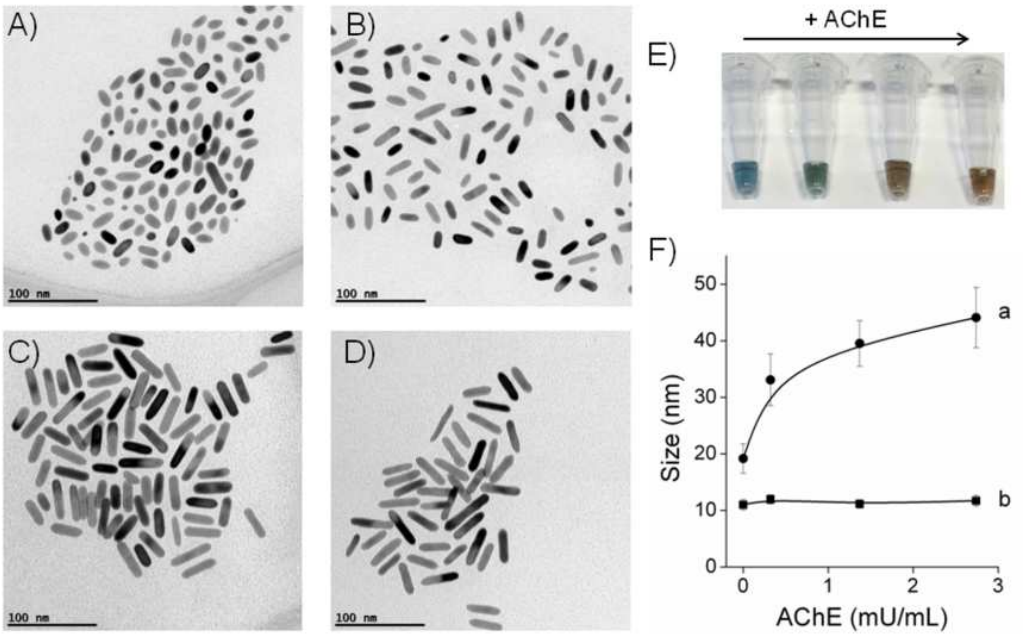

Figure 5. TEM images of the etching products obtained upon preincubation of AuNRs with 0.02 mM ATCh and varying concentrations of AChE: A) 0 mU/mL; B) 0.32 mU/mL; C) 1.37 mU/mL; D) 2.74 mU/mL. E) Colorimetric detection of AChE. (F) Length (curve **a**) and width (curve **b**) of etched AuNRs, as a function of AChE concentration. Solid lines are guides to the eye.

In Nature, AChE can be found in neuromuscular junctions and human serum. Therefore, evaluation of AChE activity in human serum allows us to determine e.g. effects of

organophosphate poisoning. With this application in mind, we validated the proposed system by running assays for the determination of AChE activity in commercially available human serum. We applied the method of standard addition, in which equal volumes of the sample serum solution were taken, all but one were separately 'spiked' with known and different amounts of AChE, and then all diluted to the same volume. The enzymatic activity of AChE was measured in all samples as described above, to determine the AChE amount in serum without the added standard. The obtained experimental LSPR positions were plotted *vs.* the concentration of added standard (Figure 6, line **a**). We also performed the enzymatic activity assay in equal volumes of aqueous buffer solution, instead of human serum, spiked with different amounts of AChE under the same experimental conditions to obtain the line **b** in Figure 6. Both lines yielded similar slopes, therefore the LSPR position corresponding to zero concentration of AChE in the buffer solution on line b (636 nm) was used as a reference point. The linear regression for human serum samples was performed to calculate the intercept of the extrapolated calibration line **a**, with the horizontal line crossing the y-axis at the reference point. This negative intercept on the reference horizontal line corresponds to the amount of the AChE in human plasma without the added standard. Taking into consideration the dilution factors of the serum samples, we computed the activity of AChE in human serum to be 2040 mU mL^{-1}, which is within the range of values reported for human plasma.[33]

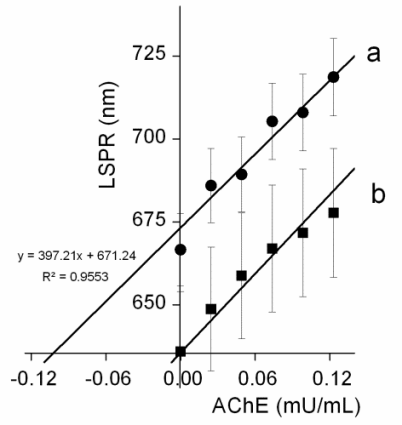

Figure 6. Quantification of AChE concentration in human serum *via* the method of standard addition. LSPR shift as a function of AChE in diluted serum (1:20000) (curve **a**) and in buffer (curve **b**). Solid lines are linear fits to the data.

Biosensing of AChE inhibitors

The protection effect of low concentrations of AChE (down to 0.1 U/L) against AuNR enzymatic etching can be exploited to develop a colorimetric assay for inhibitors of AChE activity. It is well known that nerve agents and pesticides decrease the enzymatic activity of AChE, leading to a reduction in the amount of generated thiocholine. In this case, the rate of AuNR oxidative etching increases with inhibitor concentration, ultimately leading to a blue shift of the characteristic LSPR bands. We selected two compounds paraoxon and galanthamine as model inhibitors of AChE due to their low toxicity to humans under laboratory conditions. Paraoxon (4-nitrophenyl phosphate) is an organophosphate that irreversibly inhibits AChE activity by phosphorylating the serine hydroxyl group in the active site of the enzyme [24] The assay was initiated by pre-incubation of AChE with a sample of paraoxon for 1 hour, and then the procedure for detection of active AChE after interaction with the inhibitor was applied.

Figure 7A shows the absorbance spectra of assay mixtures measured after AuNR enzymatic etching but including varying concentrations of paraoxon. The LSPR position is red-shifted as the concentration of paraoxon is increased. According to the calibration plot in Figure 7B, the detection limit was 12 nM by IUPAC definition calculated with the a confidence level of 0.95,[34] which is ca. three times lower than the detection limit demonstrated by the relevant optical assays based on AuNPs.[29, 35] A control experiment carried out within the same range of paraoxon concentrations in the absence of AChE revealed no effect of the inhibitor on the rate of AuNR enzymatic etching (data not shown). The kinetics of the irreversible inhibition of AChE by paraoxon is described by the equation:

$$[AChE]/ [AChE_0] = e^{(-k_i[I]t)} \qquad (3)$$

where [AChE] is the concentration of free active enzyme, $[AChE_0]$ is the total enzyme concentration, k_i is defined as the bimolecular rate constant and is commonly used to measure the inhibitory capacity of irreversible inhibitors, t is the time of enzyme/inhibitor interaction, [I] is the inhibitor concentration. The plot of LSPR *vs.* paraoxon concentration (**Figure 7B**) was converted into the plot of [AChE]/ $[AChE_0]$ *vs.* paraoxon concentration (**Figure 5S**) on the basis of Figure 3B. Then, the nonlinear regression analysis using equation 3 gave the value of k_i equal to 3.5×10^5 M^{-1} min^{-1}, which is the of same order of magnitude as reported in the literature. [29, 36]

Our experimental data, thus, indicate that spectral changes were caused by the specific inhibition of AChE, but neither by the inhibition of HRP nor by the adsorption of paraoxon on AuNRs.

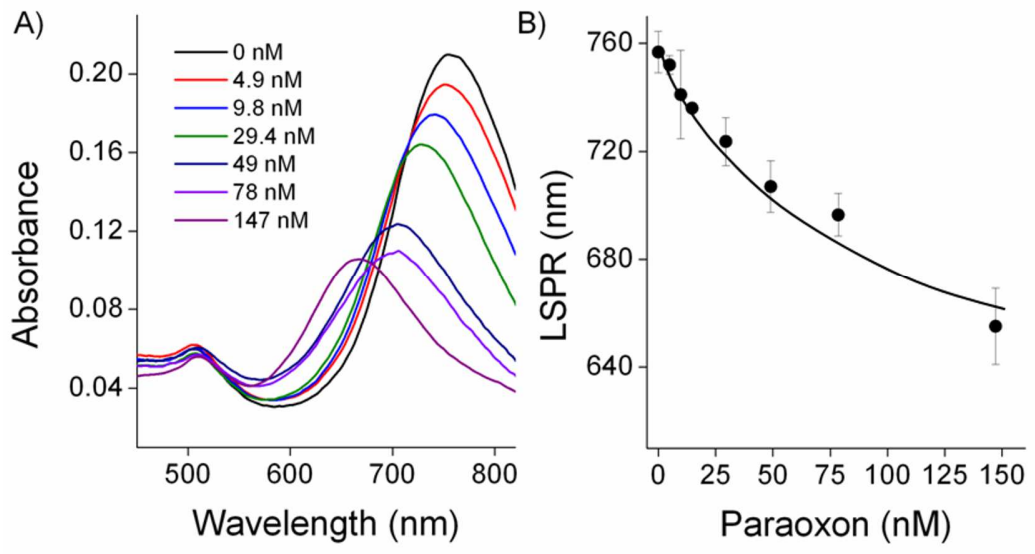

Figure 7. Inhibition of AChE activity by Paraoxon. A) Absorbance spectra of the etched AuNRs, preincubated in the presence of 0.02 mM ATCh, 1.4 mU/mL AChE and different concentrations of paraoxon. (B) LSPR shift as a function of paraoxon concentration. The solid line is a guide to the eye.

A second model inhibitor – galanthamine – is known to compete with acetylcholine for binding to the active site of AChE in a reversible manner. The assay for galanthamine was carried out by pre-incubation with AChE for 1 hour, followed by measurement of the retained enzymatic activity. **Figure 8A** shows the dependence of the absorbance spectra of resulting assay mixtures after HRP-catalyzed etching of AuNRs. The calibration plot in **Figure 8B** yields a detection limit of 40 nM by IUPAC definition calculated with the a confidence level of 0.95.[34] This detection limit was c.a. three times better than that of the previously published optical method employing inorganic NPs.[37] When AChE was absent in the assay mixture, no effect of galanthamine on the rate of AuNR enzymatic etching was detected (data not shown).

Galanthamine competes with ATCh for binding to the active site of AChE in a reversible manner, and its inhibitory mechanism is described by the equation:

$$[AChE]/[AChE_0]=[S]/(K_M^{ap}+[S]) \quad (4)$$

Where $K_M^{ap}= K_M (1 + [I]/k_i)$, k_i is the inhibitor's dissociation constant and [I] is the inhibitor concentration. The plot of $[AChE]/[AChE_0]$ *vs*. [I] (**Figure 6S** in *Supporting Information*), obtained on the basis of Figure 3B and Figure 8B, was employed in the nonlinear regression analysis using equation 4 to evaluate the value of k_i (35 nM).

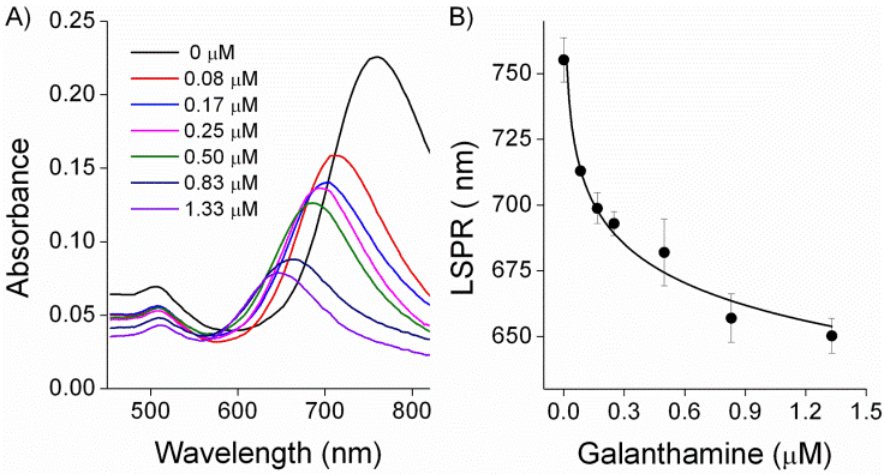

Figure 8. Inhibition of AChE activity by Galanthamine. A) Absorbance spectra of the etched AuNRs preincubated in the presence of 0.02 mM ATCh, 1.4 mU/mL AChE and different concentrations of galanthamine. (B) LSPR shift as a function of galanthamine concentration. The solid line is a guide to the eye.

Conclusions

We demonstrated that trace concentrations of the organic thiols glutathione and thiocholine are able to protect AuNRs against biocatalytic etching by HRP. According to TEM imaging, the

organic thiols modulate only the length of etched AuNRs, not affecting their width. Therefore, measurement of the longitudinal LSPR bands of AuNRs upon enzymatic etching in the presence of thiols can be employed to evaluate their binding constants to gold nanoparticles, according to the Langmuir adsorption isotherm model. We demonstrated that the concentration dependent influence of thiocholine, produced from acetylthiocholine by the enzyme AChE, on the LSPR position of etched AuNRs can be applied to develop enzymatic assays for determination of AChE and its inhibitors. In addition, we believe that the developed approach can be also employed to control the exact size of NPs of different shapes including nanorods.because the concentration of organic thiols determines the size of etched NPs. Therefore, the controlled etching is of very high importance for nanomaterials science complementing existing methods for preparation of metal NPs.

Acknowledgement

This work was supported by the Spanish Ministry of Economy and Competitiveness (project BIO2014-59741-R and MAT2013-46101-R) and Diputación Foral de Gipuzkoa program Redes 92/14.

AUTHOR INFORMATION

Corresponding Authors

*vpavlov@cicbiomagune.es; *llizmarzan@cicbiomagune.es

Author Contributions

The manuscript was written through contributions of all authors. All authors have given approval to the final version of the manuscript.

REFERENCES

1. Kelly, K. L.; Coronado, E.; Zhao, L. L.; Schatz, G. C., The optical properties of metal nanoparticles: The influence of size, shape, and dielectric environment. *J. Phys. Chem. B* **2003,** 107, 668-677.
2. Katz, E.; Willner, I., Integrated nanoparticle-biomolecule hybrid systems: Synthesis, properties, and applications. *Angew. Chem. Int. Ed. Engl.* **2004,** 43, 6042-6108.
3. Virel, A.; Saa, L.; Pavlov, V., Modulated growth of nanoparticles. Application for sensing nerve gases. *Anal. Chem.* **2009,** 81, 268-272.
4. Rodriguez-Lorenzo, L.; de la Rica, R.; Alvarez-Puebla, R. A.; Liz-Marzan, L. M.; Stevens, M. M., Plasmonic nanosensors with inverse sensitivity by means of enzyme-guided crystal growth. *Nat Mater.* **2012,** 11, 604-607.
5. Grzelczak, M.; Perez-Juste, J.; Mulvaney, P.; Liz-Marzan, L. M., Shape control in gold nanoparticle synthesis. *Chem. Soc. Rev.* **2008,** 37, 1783-1791.
6. Chen, Z.; Zhang, Z.; Qu, C.; Pan, D.; Chen, L., Highly sensitive label-free colorimetric sensing of nitrite based on etching of gold nanorods. *Analyst* **2012,** 137, 5197-5200.
7. Chen, Z.; Liu, R.; Wang, S.; Qu, C.; Chen, L.; Wang, Z., Colorimetric sensing of copper(ii) based on catalytic etching of gold nanorods. *RSC Advances* **2013,** 3, 13318-13323.
8. Saa, L.; Coronado-Puchau, M.; Pavlov, V.; Liz-Marzan, L. M., Enzymatic etching of gold nanorods by horseradish peroxidase and application to blood glucose detection. *Nanoscale* **2014,** 6, 7405-7409.
9. Coronado-Puchau, M.; Saa, L.; Grzelczak, M.; Pavlov, V.; Liz-Marzan, L. M., Enzymatic modulation of gold nanorod growth and application to nerve gas detection. *Nano Today* **2013,** 8, 461-468.
10. Perez-Juste, J.; Pastoriza-Santos, I.; Liz-Marzan, L. M.; Mulvaney, P., Gold nanorods: Synthesis, characterization and applications. *Coord. Chem. Rev.* **2005,** 249, 1870-1901.
11. Tsung, C.-K.; Kou, X.; Shi, Q.; Zhang, J.; Yeung, M. H.; Wang, J.; Stucky, G. D., Selective shortening of single-crystalline gold nanorods by mild oxidation. *J. Am. Chem. Soc.* **2006,** 128, 5352-5353.
12. Guo, X.; Zhang, Q.; Sun, Y.; Zhao, Q.; Yang, J., Lateral etching of core-shell au@metal nanorods to metal-tipped au nanorods with improved catalytic activity. *ACS Nano* **2012,** 6, 1165-1175.
13. Kou, X.; Zhang, S.; Yang, Z.; Tsung, C.-K.; Stucky, G. D.; Sun, L.; Wang, J.; Yan, C., Glutathione- and cysteine-induced transverse overgrowth on gold nanorods. *J. Am. Chem. Soc.* **2007,** 129, 6402-6404.
14. Chandrasekar, G.; Mougin, K.; Haidara, H.; Vidal, L.; Gnecco, E., Shape and size transformation of gold nanorods (gnrs) via oxidation process: A reverse growth mechanism. *Appl. Surf. Sci.* **2011,** 257, 4175-4179.
15. Lan, Y.-J.; Lin, Y.-W., A non-aggregation colorimetric method for trace lead(ii) ions based on the leaching of gold nanorods. *Anal. Methods* **2014,** 6, 7234-7242.

16. Zou, R.; Guo, X.; Yang, J.; Li, D.; Peng, F.; Zhang, L.; Wang, H.; Yu, H., Selective etching of gold nanorods by ferric chloride at room temperature. *CrystEngComm* **2009,** 11, 2797-2803.
17. Liu, X.; Zhang, S.; Tan, P.; Zhou, J.; Huang, Y.; Nie, Z.; Yao, S., A plasmonic blood glucose monitor based on enzymatic etching of gold nanorods. *Chem. Commun.* **2013,** 49, 1856-1858.
18. Li, F.-M.; Liu, J.-M.; Wang, X.-X.; Lin, L.-P.; Cai, W.-L.; Lin, X.; Zeng, Y.-N.; Li, Z.-M.; Lin, S.-Q., Non-aggregation based label free colorimetric sensor for the detection of cr (vi) based on selective etching of gold nanorods. *Sensors and Actuators B: Chemical* **2011,** 155, 817-822.
19. Busbee, B. D.; Obare, S. O.; Murphy, C. J., An improved synthesis of high-aspect-ratio gold nanorods. *Adv. Mater.* **2003,** 15, 414-416.
20. Caswell, K. K.; Wilson, J. N.; Bunz, U. H. F.; Murphy, C. J., Preferential end-to-end assembly of gold nanorods by biotin-streptavidin connectors. *J. Am. Chem. Soc.* **2003,** 125, 13914-13915.
21. Xu, L.; Kuang, H.; Xu, C.; Ma, W.; Wang, L.; Kotov, N. A., Regiospecific plasmonic assemblies for in situ raman spectroscopy in live cells. *J. Am. Chem. Soc.* **2012,** 134, 1699-1709.
22. Lee, A.; Andrade, G. F. S.; Ahmed, A.; Souza, M. L.; Coombs, N.; Tumarkin, E.; Liu, K.; Gordon, R.; Brolo, A. G.; Kumacheva, E., Probing dynamic generation of hot-spots in self-assembled chains of gold nanorods by surface-enhanced raman scattering. *J. Am. Chem. Soc.* **2011,** 133, 7563-7570.
23. Sreeprasad, T. S.; Samal, A. K.; Pradeep, T., Body- or tip-controlled reactivity of gold nanorods and their conversion to particles through other anisotropic structures. *Langmuir* **2007,** 23, 9463-9471.
24. Mileson, B. E.; Chambers, J. E.; Chen, W. L.; Dettbarn, W.; Ehrich, M.; Eldefrawi, A. T.; Gaylor, D. W.; Hamernik, K.; Hodgson, E.; Karczmar, A. G.; Padilla, S.; Pope, C. N.; Richardson, R. J.; Saunders, D. R.; Sheets, L. P.; Sultatos, L. G.; Wallace, K. B., Common mechanism of toxicity: A case study of organophosphorus pesticides. *Toxicol Sci* **1998,** 41, 8-20.
25. Liu, M.; Guyot-Sionnest, P., Mechanism of silver(i)-assisted growth of gold nanorods and bipyramids. *J. Phys. Chem. B* **2005,** 109, 22192-22200.
26. Scarabelli, L.; Sanchez-Iglesias, A.; Perez-Juste, J.; Liz-Marzan, L. M., A "Tips and tricks" Practical guide to the synthesis of gold nanorods. *J. Phys. Chem. Lett.* **2015,** 6, 4270-4279.
27. Goris, B.; Bals, S.; Van den Broek, W.; Carbo-Argibay, E.; Gomez-Grana, S.; Liz-Marzan, L. M.; Van Tendeloo, G., Atomic-scale determination of surface facets in gold nanorods. *Nat Mater.* **2012,** 11, 930-935.
28. Almora-Barrios, N.; Novell-Leruth, G.; Whiting, P.; Liz-Marzan, L. M.; Lopez, N., Theoretical description of the role of halides, silver, and surfactants on the structure of gold nanorods. *Nano Lett.* **2014,** 14, 871-875.
29. Pavlov, V.; Xiao, Y.; Willner, I., Inhibition of the acetycholine esterase-stimulated growth of au nanoparticles: Nanotechnology-based sensing of nerve gases. *Nano Lett.* **2005,** 5, 649-653.
30. Wang, M.; Gu, X.; Zhang, G.; Zhang, D.; Zhu, D., Continuous colorimetric assay for acetylcholinesterase and inhibitor screening with gold nanoparticles. *Langmuir* **2009,** 25, 2504-2507.

31. Xue, W.; Zhang, D.; Zhang, G.; Zhu, D., Colorimetric detection of glucose and an assay for acetylcholinesterase with amine-terminated polydiacetylene vesicles. *Chinese Science Bulletin* **2011,** 56, 1877-1883.
32. Li, Y.; Bai, H.; Li, C.; Shi, G., Colorimetric assays for acetylcholinesterase activity and inhibitor screening based on the disassembly-assembly of a water-soluble polythiophene derivative. *ACS Appl. Mater. Interfaces* **2011,** 3, 1306-1310.
33. Worek, F.; Mast, U.; Kiderlen, D.; Diepold, C.; Eyer, P., Improved determination of acetylcholinesterase activity in human whole blood. *Clin. Chim. Acta* **1999,** 288, 73-90.
34. McNaught, A. D., Wilkinson, A., . In *Compendium of chemical terminology. 2nd ed.* , Blackwell Scientific Publications
Oxford, 1997.
35. Sun, J.; Guo, L.; Bao, Y.; Xie, J., A simple, label-free aunps-based colorimetric ultrasensitive detection of nerve agents and highly toxic organophosphate pesticide. *Biosens. Bioelectron.* **2011,** 28, 152-157.
36. Villatte, F.; Marcel, V.; Estrada-Mondaca, S.; Fournier, D., Engineering sensitive acetylcholinesterase for detection of organophosphate and carbamate insecticides. *Biosens. Bioelectron.* **1998,** 13, 157-164.
37. Garai-Ibabe, G.; Saa, L.; Pavlov, V., Thiocholine mediated stabilization of in situ produced cds quantum dots: Application for the detection of acetylcholinesterase activity and inhibitors. *Analyst* **2014,** 139, 280-284.

ASSOCIATED CONTENT

Supporting Information. Effect of thiocholine on the rate of biocatalytic etching of gold nanorods, effect of thiols on the HRP activity, TEM images of original AuNRs and before etching and effect of inhibitor concentrations on the AChE activity. Supporting Information is available free of charge *via* the Internet at http://pubs.acs.org."

Table of Contents